Mutant mice lacking alternatively spliced p53 isoforms unveil *Ackr4* as a male-specific prognostic factor in Myc-driven B-cell lymphomas

Anne Fajac[1,2,3,4], Iva Simeonova[1,2,3,4], Julia Leemput[1,2,3,4], Marc Gabriel[2,3,4,5], Aurélie Morin[1,2,3,4], Vincent Lejour[1,2,3,4], Annaïg Hamon[1,2,3,4], Jeanne Rakotopare[1,2,3,4], Wilhelm Vaysse-Zinkhöfer[1,2,3,4], Eliana Eldawra[1,2,3,4], Marina Pinskaya[2,3,4,5], Antonin Morillon[2,3,4,5], Jean-Christophe Bourdon[6], Boris Bardot[1,2,3,4]* and Franck Toledo[1,2,3,4]*

[1]Genetics of Tumor Suppression, Institut Curie, Paris, 75248 Cedex 05, France.
[2]CNRS UMR3244, Paris, France.
[3]Sorbonne University, Paris, France
[4]PSL Research University, Paris, France.
[5]Non Coding RNA, Epigenetic and Genome Fluidity, Institut Curie, Paris, France
[6] School of Medicine, Ninewells Hospital, University of Dundee, DD1 9SY, Dundee, Scotland
* Correspondence: franck.toledo@curie.fr; boris.bardot@curie.fr.

Abstract

The *Trp53* gene encodes several isoforms of elusive biological significance. Here we show that mice lacking the *Trp53* Alternatively Spliced (AS) exon, thereby expressing the canonical p53 protein but not isoforms with the AS C-terminus, have unexpectedly lost a male-specific protection against Myc-induced B-cell lymphomas. Lymphomagenesis was delayed in $p53^{+/+}$ Eμ-Myc males compared to $p53^{\Delta AS/\Delta AS}$ Eμ-Myc males, but also compared to $p53^{+/+}$ Eμ-Myc and $p53^{\Delta AS/\Delta AS}$ Eμ-Myc females. Pre-tumoral splenic cells from $p53^{+/+}$ Eμ-Myc males exhibited a higher expression of *Ackr4*, encoding an atypical chemokine receptor with tumor suppressive effects. We identified *Ackr4* as a p53 target gene whose p53-mediated transactivation is inhibited by estrogens, and as a male-specific factor of good prognosis relevant for murine Eμ-Myc-induced and human Burkitt lymphomas. Furthermore, the knockout of *ACKR4* increased the chemokine-guided migration of Burkitt lymphoma cells. These data demonstrate the functional relevance of alternatively spliced p53 isoforms and reveal sex disparities in Myc-driven lymphomagenesis.

Keywords

p53, Ackr4, Myc, Burkitt lymphoma, sex disparity in cancer, p53 isoforms, alternative splicing, Ccl21, Ccr7

Introduction

TP53, the human gene for tumor suppressor p53, encodes several isoforms owing to distinct promoters, alternative splicing and multiple translation initiation sites (Bourdon et al., 2005; Courtois et al., 2002; Flaman et al., 1996; Yin et al., 2002). p53 alternative isoforms can be abnormally expressed in cancer cells and some may regulate the canonical p53 protein (Anbarasan and Bourdon, 2019; Bourdon et al., 2005; Mondal et al., 2013; Senturk et al., 2014). However, aberrant RNA splicing is a common feature of cancer cells (Graubert et al., 2012; Martin et al., 2013; Pajares et al., 2007; Sette and Paronetto, 2022) and to which extent alternative splicing generates functionally relevant proteins is controversial (Abascal et al., 2015; Bardot and Toledo, 2015; Blencowe, 2017; Tress et al., 2017a, 2017b; Ule and Blencowe, 2019; Weatheritt et al., 2016). Thus, the biological importance of many p53 isoforms remains elusive.

Like its human *TP53* homolog, the murine *Trp53* gene encodes multiple isoforms differing in their N- or C-termini (Arai et al., 1986; Marcel et al., 2011). Mouse models to evaluate the role of p53 isoforms differing in their N-terminus revealed that Δ40-p53 overexpression leads to accelerated ageing (Maier et al., 2004; Steffens Reinhardt et al., 2020). However, the potential role of p53 isoforms with an alternative C-terminus was not analyzed *in vivo*. p53 isoforms with distinct C-termini result from the splicing of two mutually exclusive final exons: exon 11, encoding the canonical "α" C-terminal domain, and the Alternatively Spliced (AS) exon, encoding another C-terminus (Arai et al., 1986). In adult mice, isoforms with the canonical C-terminus are predominant in all tissues (Figure S1A). Two models ($p53^{\Delta 31}$ and $p53^{\Delta CTD}$), designed to study the consequences of a loss of the canonical p53 C-terminus, exhibited signs of increased p53 activity leading to a rapidly lethal anemia (Hamard et al., 2013; Simeonova et al., 2013). To determine the role of p53-AS isoforms *in vivo*, we created $p53^{\Delta AS}$, a mouse model with a specific deletion of the AS exon (Figure S1B). In mouse embryonic fibroblasts (MEFs), the *Trp53*$^{\Delta AS}$ allele prevented the expression of isoforms with the AS C-terminus whereas it did not affect RNA levels for p53 isoforms with the canonical C-terminus (Figure S1C). We previously used this model to show that p53-AS isoforms had no role in the anemia affecting $p53^{\Delta 31/\Delta 31}$ mice (Simeonova et al., 2013). However, a detailed phenotyping of $p53^{\Delta AS/\Delta AS}$ mice remained to be performed. The detailed phenotyping, presented here, yielded surprising information on lymphomagenesis.

Results

Stress responses in WT and p53$^{\Delta AS/\Delta AS}$ cells

We analyzed cellular stress responses in thymocytes, known to undergo a p53-dependent apoptosis upon irradiation (Lowe et al., 1993), and in primary fibroblasts, known to undergo a p53-dependent cell cycle arrest in response to various stresses - e.g. DNA damage caused by irradiation or doxorubicin (Kastan et al., 1992), and the Nutlin-mediated inhibition of Mdm2, a negative regulator of p53 (Vassilev et al., 2004). We first compared thymocytes from irradiated wild-type (WT) and p53$^{\Delta AS/\Delta AS}$ mice. In WT thymocytes, isoforms with the AS C-terminus were 5 times less abundant than isoforms with the α C-terminus at the RNA level (Figure 1A), and in western blots the p53-AS protein appeared as a faint band running just ahead of, and often hard to separate from, the band specific for p53-α, the canonical full-length p53 (Figure 1B). In p53$^{\Delta AS/\Delta AS}$ thymocytes, mRNA levels for α isoforms were slightly decreased, if at all (Figure 1A), whereas p53-α protein levels appeared markedly decreased (Figure 1B), raising the possibility that p53-AS isoforms might contribute to p53-α abundance. Nevertheless, the transactivation of classical p53 target genes (Figure 1C) and apoptotic response (Figures 1D and S1D) were not significantly altered by the loss of AS isoforms. Likewise, no significant difference was observed between WT and p53$^{\Delta AS/\Delta AS}$ fibroblasts in assays for cell cycle control (Figures 1E and S1E), expression of well-known p53 target genes (Figure 1F and S1F-G), proliferation under hyperoxic conditions (Figure 1G), or the growth of tumor xenografts (Figure 1H).

Lymphomagenesis in WT and p53$^{\Delta AS/\Delta AS}$ mice

We compared spontaneous tumor onset in WT and p53$^{\Delta AS/\Delta AS}$ littermates for over 2 years and observed no significant difference in tumor-free survival (Figure 1I). Because lymphoma is a common neoplasm in C57BL6/J WT mice (Brayton et al., 2012) and our mouse cohorts resulted from >10 generations of backcrosses with C57BL6/J mice, we searched for evidence of lymphoma in the lymph nodes and spleen, by macroscopic examination at autopsy and histological analyses. B-cell lymphomas were observed in about 30% of mice of either genotype (Figure 1J). In p53$^{+/+}$ mice, a higher incidence of B-cell lymphomas was observed in females, in agreement with previous observations (Brayton et

al., 2012). By contrast, no obvious sex-specific bias was observed for B-cell lymphomas in p53$^{\Delta AS/\Delta AS}$ mice (Figure 1J), raising the possibility that the loss of p53-AS isoforms affected B-cell lymphomagenesis. However, the numbers of lymphoma-bearing mice were too small to be conclusive.

We next used Eμ-Myc transgenic mice, prone to highly penetrant B-cell lymphomas (Adams et al., 1985). p53$^{+/+}$ Eμ-Myc and p53$^{\Delta AS/\Delta AS}$ Eμ-Myc mice developed B-cell lymphomas (Figure S2A) with similar survival curves when sexes were not considered (Figure S2B). Importantly however, death was accelerated, and tumor lymph nodes were larger, in p53$^{\Delta AS/\Delta AS}$ Eμ-Myc males compared to their p53$^{+/+}$ Eμ-Myc male counterparts, whereas no difference in lymphomagenesis was noticeable between p53$^{\Delta AS/\Delta AS}$ Eμ-Myc and p53$^{+/+}$ Eμ-Myc female mice (Figure 2A-B). Our data (Figures 2A-B and S2C), together with the fact that B-cell lymphomas occur with a higher incidence in WT C57Bl6/J female mice (Brayton et al., 2012), suggested that p53$^{+/+}$ Eμ-Myc male mice are more refractory to B-cell lymphomas, and that p53-AS isoforms might confer this male-specific protection against lymphomagenesis.

Cause for accelerated lymphomagenesis in p53$^{\Delta AS/\Delta AS}$ Eμ-Myc males

We next aimed to determine the mechanisms underlying the accelerated lymphomagenesis in p53$^{\Delta AS/\Delta AS}$ Eμ-Myc males. Inactivating p53 mutations were not more frequent in tumors from p53$^{\Delta AS/\Delta AS}$ Eμ-Myc males than in those from p53$^{+/+}$ Eμ-Myc males, ruling out additional mutations at the *Trp53* locus as potential causes for accelerated lymphomagenesis in p53$^{\Delta AS/\Delta AS}$ Eμ-Myc males (Figures S2D-E). We next analyzed a subset of tumors with no detectable *Trp53* mutation in males of both genotypes and found that Myc was expressed at similar RNA and protein levels in all tumors (Figure 2C). No difference in p53-α mRNA levels was observed in tumors from both genotypes, although a decrease at the protein level was detected in most tumors from p53$^{\Delta AS/\Delta AS}$ Eμ-Myc males (Figure 2D). Nevertheless, similar transcript levels for classical p53 target genes were observed in tumor cells of both genotypes (Figure 2E). To test whether a higher tumor volume in p53$^{\Delta AS/\Delta AS}$ Eμ-myc males might result from lower apoptosis and/or higher cell proliferation, we next analyzed tumors by immunohistochemistry with antibodies against cleaved caspase-3 or ki-67, respectively. Similar apoptotic and proliferation indexes were observed for both genotypes (Figure 2F-G). In sum, classical assays for p53 activity in tumors failed to account for differences between the two male genotypes.

The speed of lymphomagenesis in Eμ-Myc mice correlates with the extent of B-cell expansion in the first stages of B cell differentiation (Langdon et al., 1986) and p53 was proposed to control the pool of early B cells (Slatter et al., 2010). Therefore, we determined the levels of the early pre-B / immature B cells in 6 weeks-old mice, before any sign of tumor. We analyzed the spleen, a preferential site of B-cell expansion (Langdon et al., 1986) with a relatively high AS/α isoform ratio (Figure S1A). Flow cytometry with a combination of markers was used to discriminate the pre-B, immature, transitional and mature B subpopulations. As expected (Langdon et al., 1986), we observed high numbers of pre-B and immature B cells in Eμ-Myc mice. In males, pre-B and immature B cells were more abundant in $p53^{\Delta AS/\Delta AS}$ Eμ-Myc animals, while no difference was observed for transitional and mature B cells (Figures 3A and S3A). By contrast, in the spleen of $p53^{+/+}$ and $p53^{\Delta AS/\Delta AS}$ 6 weeks-old male mice without the Eμ-Myc transgene, most B cells were mature B cells (Figure S3B). In Eμ-Myc females, the numbers of pre-B and immature B cells were similar between genotypes, as were the numbers of transitional and mature B cells (Figure 3A). Interestingly, $p53^{+/+}$ Eμ-myc males, which develop lymphomas less rapidly, exhibited the lowest number of immature B cells (Figure 3A), suggesting a direct correlation between the level of immature B cell expansion and the speed of lymphomagenesis. Together, these data suggested that p53-AS isoforms may not be required to control the pool of early B cells under normal conditions, but that in an Eμ-Myc context they would limit the expansion of pre-tumor early B cells, specifically in males.

Transcriptomes from $p53^{+/+}$ Eμ-Myc and $p53^{\Delta AS/\Delta AS}$ Eμ-Myc male spleens

We next performed bulk RNA-seq and differential expression analyses comparing the spleens from 4-6 weeks-old $p53^{\Delta AS/\Delta AS}$ Eμ-Myc males to spleens from age-matched $p53^{+/+}$ Eμ-Myc males. This revealed a limited number of significantly deregulated genes (Figure 3B), including 13 protein-coding genes and 11 pseudogenes (Figure 3C). Out of the 13 protein-coding genes, we focused on the 10 genes not encoding an immunoglobulin and analyzed the same samples by RT-qPCR (Figure 3D). For 6 of the 10 genes, expression levels were too low to be quantified (*Tcstv3*), or differences in expression were not statistically significant (*Masp2*, *Akr1c19*, *Cd300lh*, *Il5ra*, *Slc26a1*). Of note, *Il5ra* belonged to this group, although it is regulated by p53 (Zhu et al., 2022), which illustrates the difficulty to analyze subtle effects in our experiments. Taking this into account, we considered as potentially interesting the 4 remaining genes, exhibiting differences in mRNA

levels with statistical significance ($p<0.05$) or borderline statistical significance ($p=0.057$): *Ackr4*, less expressed in $p53^{\Delta AS/\Delta AS}$ Eμ-Myc males, and *Fam132a*, *Mt2* and *Prss50*, with an increased expression in $p53^{\Delta AS/\Delta AS}$ Eμ-Myc males (Figure 3D). Importantly, survival curves indicated that the Myc-induced lethality was delayed in $p53^{+/+}$ Eμ-Myc males compared to $p53^{\Delta AS/\Delta AS}$ Eμ-Myc males, $p53^{+/+}$ Eμ-Myc females and $p53^{\Delta AS/\Delta AS}$ Eμ-Myc females (Figure S2C). Thus, we quantified transcripts for *Ackr4*, *Fam132a*, *Mt2* and *Prss50* in the spleen of 4-6 weeks-old $p53^{+/+}$ Eμ-Myc and $p53^{\Delta AS/\Delta AS}$ Eμ-Myc females, then compared mRNA levels in $p53^{+/+}$ Eμ-Myc males versus the 3 other groups. Significantly higher expression of *Ackr4* and lower expression of *Mt2* were found in $p53^{+/+}$ Eμ-Myc males (Figure 3E).

Ackr4 (also known as *Ccrl1*) encodes the atypical chemokine receptor 4, a decoy receptor promoting the degradation of chemokines that modulate cancer cell proliferation and metastasis (Chow and Luster, 2014; Marcuzzi et al., 2018; Müller et al., 2001). Our data suggested that *Ackr4* might be a gene transactivated by p53-α and/or p53-AS isoforms. Consistent with this, by extracting data from a transcriptome-wide study in MEFs (Younger et al., 2015) we found evidence for a p53-dependent transactivation of *Ackr4* in response to doxorubicin (Figure 3F). Furthermore, ChIP-Atlas, the database of chromatin immunoprecipitation experiments (Oki et al., 2018), indicated p53 binding to sequences within the intron 1 of *Ackr4* in doxorubicin-treated MEFs, and we identified a candidate p53 responsive element in this intron (Figure 3G). We next used luciferase assays to show that this p53 responsive element can be bound and regulated by both p53-α and p53-AS (Figures 3G-H and S3C). Together, these data show that *Ackr4* is indeed a p53 target gene, although RNAseq data indicated that it is expressed at much lower levels than classical p53 targets like *Cdkn1a* or *Mdm2* in the splenic cells of Eμ-Myc mice (Table S1). Furthermore, *Ackr4* was shown to be regulated by Foxl2 and estrogen signalling in ovarian cells (Georges et al., 2014) and 17-β estradiol was recently found to regulate *ACKR4* expression in meniscal cells from both sexes, albeit differentially (Knewtson et al., 2020). Accordingly, we observed, in both WT and $p53^{\Delta AS/\Delta AS}$ MEFs, that p53 activation with the Mdm2 antagonist Nutlin led to the transactivation of *Ackr4*, but that a concomitant treatment with 17-β estradiol markedly decreased, or completely abrogated, *Ackr4* transactivation (Figure 3I). By contrast, *Cdkn1a* was efficiently transactivated under both conditions in mutant and WT cells (Figure 3I). These data indicate that *Ackr4* is a p53 target gene whose p53-mediated transactivation can be inhibited by estrogens.

The *Mt2* gene, encoding the potentially oncogenic metallothionein-2 (Si and Lang, 2018), was less expressed in p53$^{+/+}$ Eμ-Myc male pre-tumoral splenic cells, which raised the possibility of its direct or indirect repression by p53, potentially through the binding of p53 or the DREAM complex at its promoter (Engeland, 2018; Peuget and Selivanova, 2021). However, ChIP-Atlas reported no binding of these proteins at the *Mt2* promoter. Alternatively, evidence that Myc may impact on *Mt2* expression was obtained previously (Qin et al., 2021), and ChIP-Atlas reported Myc binding at the *Mt2* promoter in primary B-cells from lymph nodes of Eμ-Myc mice as well as Eμ-Myc-induced lymphoma cells (Figure 3J). This may suggest that the lower expression of *Mt2* in pre-tumoral splenic cells from p53$^{+/+}$ Eμ-Myc males (Figure 3E) might result from a subtle difference in Myc signalling. Consistent with this, the comparison of transcriptomes of splenic cells from p53$^{\Delta AS/\Delta AS}$ Eμ-Myc males and p53$^{+/+}$ Eμ-Myc males, when analyzed by gene set enrichment analysis (Subramanian et al., 2005), revealed an enrichment of hallmark Myc target genes in p53$^{\Delta AS/\Delta AS}$ Eμ-Myc male splenic cells (Figure 3K, Table S2).

Relevance of *ACKR4* expression in Burkitt lymphomas

Murine and human alternatively spliced p53 isoforms exhibit structural differences (Marcel et al., 2011) and the ChIP-Atlas database (Oki et al., 2018) does not report p53 binding to the human *ACKR4* intron 1. Nevertheless, we found that p53 activation in human cells also led to an increased *ACKR4* expression abrogated by 17-β estradiol, whereas 17-β estradiol had no significant effect on the p53-mediated transactivation of *CDKN1A* (Figure 4A). This led us to investigate the potential relevance of *ACKR4* expression in human B-cell lymphomas. We analyzed public databases of B-cell lymphomas patients with clinical and gene expression information. We first analyzed #GSE4475 (Hummel et al., 2006), a dataset of mature aggressive B-cell lymphomas previously used to define Burkitt lymphoma-like specific transcriptomes, comprising 159 patients (91 men, 68 women) with clinical follow-up. Overall, *ACKR4* gene expression was not significantly different between male and female patients (Figure 4B, left). However, average mRNA levels appeared higher in males when we considered the 30% patients of each sex with the highest *ACKR4* expression (Figure 4B, right). Strikingly, when we compared the survival of 30% patients with the highest ACKR4 mRNA levels to the survival of the 30% patients with the lowest ACKR4 mRNA levels, high *ACKR4* expression correlated with a better prognosis in men, but not in women (Figure 4C). By contrast, for *MT2A*, the human homolog of *Mt2*, differences in

mRNA levels did not correlate with significant differences in survival for either sex (Figure S4A).

We also analyzed dataset #GSE181063 (Lacy et al., 2020), comprising mostly diffuse large B-cell lymphomas (DLBCL; 613 men, 536 women) and a few Burkitt lymphomas (65 men, 18 women). We found no difference in survival curves of DLBCL patients with low versus high *ACKR4* levels, neither in men nor in women. However, there was again an increased survival for Burkitt lymphoma male patients with high *ACKR4* expression, but not for women (Figure S4B). Next, we analyzed #phs000235 (Morin et al., 2011), a Burkitt lymphoma-specific dataset (65 men, 37 women) comprising mostly patients diagnosed at 0-17 years of age, hence providing cohorts homogeneous for both tumor type and age of onset. Again, *ACKR4* was expressed at higher levels in a subset of male patients (Figure 4D) and high *ACKR4* expression correlated with a better prognosis only in males (Figure 4E). Finally, we analyzed dataset #GSE136337 (Danziger et al., 2020), comprising data from the malignant plasma cells of patients with multiple myeloma (260 men, 166 women), and found that *ACKR4* is not a prognostic factor for this cancer type (Figure S4C). Altogether, these analyses led us to conclude that, as in Eμ-Myc mice, *ACKR4* is a male-specific positive prognostic factor in Burkitt lymphoma, the archetype of MYC-driven B-cell lymphomas.

We next considered the possibility that ACKR4 might be more than a biomarker, if it acts as a suppressor of MYC-driven B-cell lymphomagenesis. In support of this hypothesis, ACKR4 scavenges the chemokine CCL21, a ligand of the chemokine receptor CCR7 (Bastow et al., 2021; Ulvmar et al., 2014), and the ACKR4-mediated sequestration of CCL21 may impair the CCR7 signalling cascade, which might lead to decreased MYC activity (Shi et al., 2015). Consistent with this, a *Ccr7* deficiency was shown to delay the lymphomagenesis induced by Eμ-Myc in mice (Rehm et al., 2011). In addition, Ccr7 is required for lymphoma cell lodging to secondary lymphoid organs (Rehm et al., 2011) and ACKR4 expression was inversely correlated with the metastasis capacity of different types of cancer cells (Shi et al., 2015; Zhu et al., 2014). These data suggested that ACKR4 might regulate the behavior of Burkitt lymphoma cells. To test this hypothesis, we designed a CRISPR-Cas9 approach to perform the knockout of *ACKR4* in Raji cells. Raji is a Burkitt lymphoma cell line isolated from a 11 years-old male patient (Pulvertaft, 1964). Although p53 is mutated in Raji cells (Duthu et al., 1992), these cells overexpress MYC (Hamlyn and Rabbitts, 1983) and express both ACKR4 and CCR7 (Ferreira et al., 2014), suggesting that

they might be suitable to evaluate the impact of ACKR4 on Burkitt lymphoma cell behavior, particularly their migratory capacities. Raji cells were transfected with a vector expressing Cas9, a puromycin resistance gene and either of two guide RNAs targeting *ACKR4* (or no guide RNA for control), then puromycin-resistant cells were selected and recovered as cellular pools or diluted to isolate cellular clones (Figure S5). Both guide RNAs targeted sequences in *ACKR4* mapping upstream an encoded DRY motif essential for signal transduction (Watts et al., 2013), so that Cas9-induced DNA breaks would generate knockout alleles. With this strategy, we obtained puromycin-resistant clones from Raji cells, two of which were verified to be *ACKR4* KO clones by DNA sequencing (Figure S6). We compared the proliferation and migration capacities of Raji control cells (transfected with the Cas9 expression vector without guide RNAs) and the two independent *ACKR4* KO Raji clones identified, cultured for 15 hours in medium supplemented or not with the CCL21 chemokine. Under these conditions, Raji cells of all genotypes appeared to proliferate similarly (Figure S7). Strikingly however, the KO of *ACKR4* led to a 4-fold increase in CCL21-mediated cell migration, consistent with the hypothesis that ACKR4 may hinder MYC-driven B-cell lymphomagenesis (Figure 4F).

Discussion

In this report we analyzed a mouse model with a specific deletion of the alternatively spliced (AS) exon of the *Trp53* gene. Despite a subtle phenotype, this model revealed that a male-specific protective effect against Eμ-Myc-induced B-cell lymphomas is lost in the absence of p53-AS isoforms. $p53^{\Delta AS/\Delta AS}$ males also appeared more prone to develop spontaneous lymphomas, suggesting that the sex-specific protective effect conferred by p53-AS isoforms might not be restricted to the Eμ-Myc model.

Our transcriptomic data from splenic cells of $p53^{+/+}$ Eμ-Myc and $p53^{\Delta AS/\Delta AS}$ Eμ-Myc males disclosed very few differentially expressed genes, and highlighted *Ackr4* as a male-specific positive prognostic factor in Eμ-Myc-induced lymphomas. Mechanistically, we identified *Ackr4*, expressed at low levels in splenic cells, as a p53 target gene that may be transactivated by p53-α and/or p53-AS according to luciferase assays. That *Ackr4* might be regulated by both types of p53 isoforms was expected, because their DNA binding domains are identical. In fact, if one considers that p53-α isoforms appear more abundant than p53-AS isoforms in wild-type cells, and that the loss of p53-AS isoforms correlated with a decrease in p53-α levels in the thymocytes and tumor lymph nodes of mutant mice, then it seems likely that the reduced transactivation of *Ackr4* in the splenic cells of $p53^{\Delta AS/\Delta AS}$ Eμ-Myc males could mainly result from decreased p53-α levels, rather than the loss of p53-AS isoforms *per se*. In addition, we observed that 17-β estradiol can inhibit the p53-mediated transactivation of *Ackr4*. Together, our data suggest that *Ackr4* may be regulated by p53-α, p53-AS and estrogens, likely accounting for sex-specific and p53-status dependent differences in gene expression.

Our analyses reveal that in both mice and humans, *Ackr4/ACKR4* is a male-specific prognostic factor in Burkitt-like lymphomas. Furthermore, several lines of evidence suggest that Ackr4 might act as a tumor suppressor of Myc-driven B-cell lymphomas. As mentioned before, the ACKR4-mediated sequestration of CCL21 may impair the CCR7 signalling cascade, which might lead to decreased MYC activity (Shi et al., 2015). In $p53^{+/+}$ Eμ-Myc male splenic cells, the observed lower expression of *Mt2*, known to be regulated by Myc (Qin et al., 2021), and of many genes that are hallmark Myc targets (as revealed by GSEA), appear consistent with this hypothesis. In addition, Ccr7 is required for lymphoma cell lodging to secondary lymphoid organs (Rehm et al., 2011) and ACKR4 expression was inversely correlated with the metastasis capacity of different types of cancer cells (Shi et al.,

2015; Zhu et al., 2014). Consistent with this, we found that the KO of *ACKR4* in Raji Burkitt lymphoma cells led to a dramatic increase in CCL21-guided cell migration. Finally, Ackr4 regulates B cell differentiation (Kara et al., 2018), which raises the possibility that an alteration of the p53-Ackr4 pathway in $p53^{\Delta AS/\Delta AS}$ Eμ-Myc male splenic cells might contribute to increase the pools of pre-B and immature B cells that may be prone to lymphomagenesis. In sum, a decrease in Ackr4 expression might promote B-cell lymphomagenesis through several non-exclusive mechanisms. Importantly, ACKR4 was previously found to inhibit the growth and metastasis of breast, cervical, colorectal, hepatocellular and nasopharyngeal cancer cells (Feng et al., 2009; Hou et al., 2013; Ju et al., 2019; Shi et al., 2015; Zhu et al., 2014), although no report mentioned any sex-specific bias for cancers occurring in both sexes. Our data provide evidence that sex-specific differences in *Ackr4* expression may have prognostic value. This suggests that measuring *ACKR4* gene expression in male patients with Burkitt lymphoma could be useful to identify the patients at higher risk, for whom specific therapeutic regimens might be required.

Interestingly, our data suggested that *Mt2* might be a male-specific negative prognostic factor in murine Eμ-Myc induced lymphomas, but *MT2A* expression levels had no prognostic value in human lymphomas. A possible explanation for this discrepancy is suggested by the fact that *Mt2* is regulated by Myc. A translocation leading to MYC overexpression drives oncogenesis in all Burkitt lymphomas, but half of them exhibit additional missense MYC mutations enhancing its tumorigenicity (Chakraborty et al., 2015). The transcriptional program of a WT and two lymphoma-associated Myc mutants were recently compared, and we noticed that one of the mutants led to an alteration in *Mt2* expression (Mahani et al., 2021), which would abrogate any potential prognostic value.

Finally, a polymorphism in the *MDM2* gene promoter provided evidence that sex-specific hormones may affect p53 signalling and tumorigenesis (Bond and Levine, 2007). More recently, a higher frequency of *TP53* mutations in men, together with an increased vulnerability to alterations of X-linked genes encoding p53 regulators, were proposed to explain a higher cancer incidence and death in male patients (Haupt et al., 2019). Here, on the contrary, male mice and a subset of male patients were more efficiently protected against Burkitt-like lymphomas, which adds another layer of complexity to sex-specific differences in tumorigenesis. The p53 pathway thus underlies cancer sex-disparities through multiple mechanisms, that may notably include variations in p53 isoforms or Ackr4 expression.

Materials and Methods

Mice

Design and construction of the $p53^{\Delta AS}$ mouse model was previously described (Simeonova et al., 2013). A minimum of 10 backcrosses with C57Bl6/J mice of both sexes (Charles River Laboratories) were performed before establishing the cohorts of $p53^{+/+}$ and $p53^{\Delta AS/\Delta AS}$ littermate mice used in this study. Mouse genotyping with multiple primer sets confirmed >99% C57Bl6/J genetic background after 10 backcrosses (primer sequences available upon request). Cohorts of $p53^{+/+}$ Eμ-Myc and $p53^{\Delta AS/\Delta AS}$ Eμ-Myc mice were established with identical parental origin of the Eμ-Myc transgene. For all experiments, mice housing and treatment were conducted according to Institutional Animal Care and Use Committee of the Institut Curie.

Cells and cell culture reagents

Mouse embryonic fibroblasts (MEFs) were isolated from 13.5 days post-coitum embryos and cultured in a 5% CO_2 and 3% O_2 incubator, in DMEM Glutamax (Gibco), with 15% FBS (PAN Biotech), 100 μM 2-mercaptoethanol (Millipore), 0.1 mM Non-Essential Amino-Acids and penicillin/streptomycin (Gibco) for less than 5 passages, except for 3T3 experiments, performed in a 5% CO_2 incubator for 9 passages. Cells were treated for 24h with 0.5 μg/ml Doxorubicin (Sigma-Aldrich), 15 μM Etoposide (Sigma-Aldrich), 10 μM Nutlin 3a (Vassilev et al., 2004) (Sigma-Aldrich) and/or 5 μg/ml 17β-Estradiol (Merck). At least 3 independent experiments with at least 2 independent littermate MEF clones of each genotype and each sex were performed to measure DNA damage responses. For estradiol assays, four independent experiments with three independent MEF male clones of each genotype were performed. Human lung fibroblast MRC5 and its SV40-transformed derivatives were cultured in a 5% CO2 and 3% O2-regulated incubator in MEM medium without Phenol Red (Gibco), completed with 10% FBS, 2 mM L-glutamine (Gibco), 1 mM pyruvate, 0.1 mM Non-Essential Amino-Acids, and penicillin/streptomycin, and treated for 24h with 10 μM Nutlin 3a and/or 5 μg/ml 17β-Estradiol (Merck). Four independent experiments were performed. Burkitt lymphoma cells (Raji or Raji *ACKR4* KO derivatives) were cultured in a 5% CO2 incubator in RPMI Glutamax (Gibco) supplemented with 10% FBS, 2 mM L-glutamine, 1 mM pyruvate, 0.1 mM Non-Essential Amino-Acids, 0.45% glucose (Sigma-Aldrich), and penicillin/streptomycin. In proliferation and migration assays, Raji control cells

and two independent *ACKR4* KO derivatives were treated or not for 15h with 1 μg/ml CCL21 (PreproTech) then counted in triplicates.

Quantitative RT-PCR

Total RNAs were extracted using nucleospin RNA II (Macherey-Nagel), reverse-transcribed using superscript IV (Invitrogen), and real-time quantitative PCRs were performed on an ABI PRISM 7500 using Power SYBR Green (Applied Biosystems) as previously described (Simeonova et al., 2012). For quantification of p53 isoforms in healthy tissues, a forward primer in exon 10 and a reverse primer encompassing the boundary between exons 10 and 11 were used for p53-α amplification, whereas the same forward primer and a reverse primer located in exon AS were used for p53-AS amplification (see Table S3 for primer sequences). To determine the AS/α mRNA ratios, expression levels were compared with a standard curve generated by serial dilutions of a plasmid containing both p53-AS and p53-α cDNAs.

Western blots

Thymocytes were lysed in RIPA buffer (50 mM Tris-HCl pH 8, 150 mM NaCl, 5 mM EDTA, 0.5% deoxycholic acid, 0.1% SDS, 1% NP-40) with a cocktail of protease inhibitors (Roche) and 1 mM PMSF (Sigma). Whole-cell extracts were sonicated three times for 10 s and centrifuged at 13 000 r.p.m. for 30 min to remove cell debris. MEFs or B-cell lymphomas were lysed in Giordano's buffer (50 mM Tris-HCl pH 7.4, 250 mM NaCl, 5 mM EDTA, 0.1% Triton X-100) with a cocktail of protease inhibitors (Roche) and 1 mM PMSF (Sigma). Protein lysate concentration was determined by BCA assay (Thermo Scientific) and 30 μg of each lysate was fractionated by SDS–PAGE on a 4-12% polyacrylamide gel and transferred onto PDVF membrane (Amersham). Membranes were incubated with antibodies against p53 (CM5, Novocastra), myc (9E-10, Santa Cruz), p21 (F-5, Santa Cruz) and actin (actin-HRP sc47778, Santa Cruz) and revealed with SuperSignal West femto detection reagent (Thermo Scientific).

Apoptosis Assays

Six weeks-old $p53^{+/+}$ and $p53^{\Delta AS/\Delta AS}$ male mice were whole-body irradiated with 5 Gy of γ-irradiation. Mice were sacrificed 4h later and thymocytes were recovered, stained with

AnnexinV-FITC Apoptosis detection kit (Abcam), then analyzed by flow cytometry using FlowJo.

Cell-Cycle assays

Log phase MEFs were irradiated at room temperature with a CS γ-irradiator at doses of 3 or 10 Gy, incubated for 24h, then pulse-labeled for 1h with 10 μM BrdU, fixed in 70% ethanol, double-stained with FITC anti BrdU and propidium iodide, and sorted by flow cytometry using a BD FACSort. Data were analyzed using FlowJo.

Oncogene-induced tumor xenografts

MEFs with the indicated genotypes were sequentially infected with pWZL-E1A12S and pBABE-Hrasv12 viruses as previously described (Toledo et al., 2006). In total, $5x10^6$ E1A- and Ras- (E1A+Ras) expressing MEFs of each genotype were injected subcutaneously into the flanks of 7-weeks-old female athymic nude mice (at least 4 mice per genotype) and tumor volumes were determined 1, 8, 15, 21 and 25 days after injection. Importantly, populations of (E1A+Ras)-expressing cells were used to minimize potential differences in expression levels that could result from independent viral insertion sites.

Cell sorting of B-cell sub-populations

Splenic cells were recovered from 6 weeks-old asymptomatic mice and incubated with DAPI and the following antibodies: APC rat anti-mouse CD45R/B220, FITC rat anti-mouse CD43, PE rat anti-mouse IgM and BV605 rat anti-mouse IgD (BD Pharmingen). First, the B220+CD43- cells were selected by flow cytometry from DAPI negative living cells, yielding subsequently 4 different B subpopulations based on IgM and IgD labeling: IgM-/IgD- preB lymphocytes, IgM low/IgD- immature B lymphocytes, IgM high/IgD- transitional B lymphocytes and IgM+/IgD+ mature B lymphocytes.

RNA-Seq analysis

Total RNA was extracted from the spleen of 4-6 weeks-old asymptomatic mice using nucleospin RNA II (Macherey-Nagel). The quality of RNA was checked with Bioanalyzer Agilent 2100 and RNAs with a RIN (RNA integrity number) $\geq$ 6 were retained for further analysis. RNA was depleted from ribosomal RNA, then converted into cDNA libraries using a TruSeq Stranded Total Library preparation kit (Illumina). Paired-end sequencing was performed on an Illumina MiSeq platform. Reads were mapped to the mouse genome

version GRCm38 and counted on gene annotation gencode.vM18 with featureCounts (Liao et al., 2014). Differentially expressed genes of C57Bl6/J genetic background with an adjusted p-value < 0.05 were identified using the DESeq2 R package (Love et al., 2014). Gene set enrichment analysis was performed by using the GSEA software with canonical pathway gene sets from the Mouse Molecular Signature Database (MSigDB) (Subramanian et al., 2005).

Luciferase assays

The candidate p53 responsive element (p53 RE) in the *Ackr4* promoter was identified by using the JASPAR database of binding profiles (Fornes et al., 2020) with the position weight matrix scanner PWMscan (Ambrosini et al., 2018). A 1.5 kb fragment from *Ackr4* intron 1, containing a WT or mutant p53 RE at its center, was cloned upstream a SV40 minimal promoter and a luciferase reporter gene in the backbone of a PGL3 plasmid (Promega). We used lipofectamine 2000 to transfect $p53^{-/-}$ MEFs with 2 μg of either luciferase expression vector, 2 μg of an expression vector for $p53^{WT}$, $p53^{AS}$ or the DNA-binding mutant $p53^{R270H}$, and 30 ng of a renilla luciferase expression plasmid (pGL4.73, Promega) for normalization. Transfected cells were incubated for 24 h then trypsinized, resuspended in 75 μl culture medium with 7.5% FBS and transferred into a well of an optical 96-well plate (Nunc). The dual-glo luciferase assay system (Promega) was used according to the manufacturer's protocol to lyse the cells and read firefly and renilla luciferase signals. Results were normalized, then the average luciferase activity in cells transfected with the WT p53RE luciferase reporter and the $p53^{R270H}$ expression plasmid were assigned a value of 1.

Generation of *ACKR4* Knockout Burkitt lymphoma cells

Six guide RNAs (gRNAs) were designed to target the human *ACKR4* gene by using the web tool CRISPOR (Haeussler et al., 2016). For each gRNA, two reverse complementary oligonucleotides were designed (with added backbone sequences, including a 5′ G nucleotide for gRNA sequences without a 5′ G to improve transcription efficiency from a U6 promoter), annealed and cloned in the Cas9 expression vector pSpCas9(BB)-2A-Puro (PX459) (Addgene). Prelimary tests for efficiency to induce cleavage in the targeted DNA regions were performed in HEK293T cells, which led to select the gRNAs #4 (5'-TGGTAGTGGCAATTTATGCC-3') and #5 (5'-GGGCTGTTAATGCAGTTCAT-3') for further experiments. Raji Burkitt lymphoma cells were transfected with a PX459 vector expressing gRNA #4 or #5 (or no gRNA for control), by using Nucleofector Amaxa kit V

(Lonza), and selection was carried out with 1 μg/ml puromycin for 3 weeks to obtain stably transfected cells. Clones were obtained by seeding cells at low density (1 cell/5 wells) in 96-well plates, expanded, then subdivided in two parts, half for storage in liquid nitrogen and half for *ACKR4* genotyping by Sanger DNA sequencing (see Table S3 for primer sequences). For each cell clone, the *ACKR4* target DNA regions were amplified by PCR, PCR products were cloned in a PGL3 plasmid, and 8 transformed bacteria colonies were sequenced (Figure S5). This led to identify two homozygous *ACKR4* KO clones, one (clone 4.14) obtained by using gRNA #4 and one (clone 5.2) by using gRNA #5 (Figure S6).

Cell migration assay

Cell migration assys towards the chemokine CCL21 were performed with Boyden chambers essentially as described (Calpe et al., 2011), by measuring transwell migration across bare polycarbonate membranes with a pore size of 5 μm (Corning). A total of 100 μl of culture medium (RPMI Glutamax, 10% FBS, 2 mM L-glutamine, 1 mM pyruvate, 0.1 mM Non-Essential Amino-Acids, 0.45% glucose, and penicillin/streptomycin) containing $5x10^5$ cells was added to a 6.5 mm diameter transwell insert, and 600 μl of culture medium with or without 1μg/ml CCL21 were added to the lower compartment. After 15h at 37°C in 5% CO2, the number of migrated cells in the lower chamber was determined by using a Coulter Counter.

Statistical Analyses

Student's unpaired *t* tests were used in most Figures to analyze differences between WT vs ΔAS values. Log-Rank (Mantel-Cox) tests were used to analyze Kaplan-Meier tumor-free survival curves. Analyses were performed using Graphpad Prism 5, and values of $p<0.05$ were considered significant.

Data availability

RNA sequencing data have been deposited in the Gene Expression Omnibus (GEO) under the accession code GSE209708.

Acknowledgments

This project was supported by grants from the Comité Tumeurs of Fondation de France (to F.T.), the Comité Ile-de-France and Comité national (Labellisation 2014-18) of the Ligue Nationale Contre le Cancer (to F.T.), and the Fondation ARC pour la recherche sur le Cancer (to F.T.). I.S., J.R. and E.E. were PhD fellows of the Ministère de la Recherche; J.L. and A.M. were post-doctoral fellows of Cancéropôle Ile-de-France and Institut National du Cancer. M.G. was paid by European Research Council 875532-Prostator-ERC-2019-PoC attributed to A.M.; J.C.B. was supported by Cancer Research-UK. We thank K. Fernandes for his participation in making the ΔAS mutation, and members of the Institut Curie platforms: I. Grandjean, H. Gautier, C. Daviaud, M. Garcia, M. Verlhac, A. Fosse and P. Bureau (animal facility); S. Baulande and S. Lameiras (NGS); M. Huerre, A. Nicolas and R. Leclere (histopathology); Z. Maciorowski, A. Viguier and S. Grondin (flow cytometry).

Author Contributions

F.T, J.C.B. and I.S. initiated the project; F.T., B.B. and A.F. designed the research and analyzed data; B.B., A.F., I.S., J.L., A.M., V.L., F.T., A.H., J.R., W.V.-Z. and E.E. performed the research; M.G., B.B., M.P. and A.M. analyzed RNAseq data; F.T. acquired funding; F.T., A.F. and B.B. wrote the paper.

Declaration of interests

The authors declare no competing interest.

References

Abascal F, Ezkurdia I, Rodriguez-Rivas J, Rodriguez JM, del Pozo A, Vázquez J, Valencia A, Tress ML. 2015. Alternatively Spliced Homologous Exons Have Ancient Origins and Are Highly Expressed at the Protein Level. *PLoS Comput Biol* **11**:e1004325. doi:10.1371/journal.pcbi.1004325

Adams JM, Harris AW, Pinkert CA, Corcoran LM, Alexander WS, Cory S, Palmiter RD, Brinster RL. 1985. The c-myc oncogene driven by immunoglobulin enhancers induces lymphoid malignancy in transgenic mice. *Nature* **318**:533–538. doi:10.1038/318533a0

Ambrosini G, Groux R, Bucher P. 2018. PWMScan: a fast tool for scanning entire genomes with a position-specific weight matrix. *Bioinformatics* **34**:2483–2484. doi:10.1093/bioinformatics/bty127

Anbarasan T, Bourdon J-C. 2019. The Emerging Landscape of p53 Isoforms in Physiology, Cancer and Degenerative Diseases. *Int J Mol Sci* **20**:E6257. doi:10.3390/ijms20246257

Arai N, Nomura D, Yokota K, Wolf D, Brill E, Shohat O, Rotter V. 1986. Immunologically distinct p53 molecules generated by alternative splicing. *Mol Cell Biol* **6**:3232–3239. doi:10.1128/mcb.6.9.3232-3239.1986

Bardot B, Toledo F. 2015. Mdm4: don't judge an isoform by its mRNA levels! *Aging (Albany NY)* **7**:744–745. doi:10.18632/aging.100826

Bastow CR, Bunting MD, Kara EE, McKenzie DR, Caon A, Devi S, Tolley L, Mueller SN, Frazer IH, Harvey N, Condina MR, Young C, Hoffmann P, McColl SR, Comerford I. 2021. Scavenging of soluble and immobilized CCL21 by ACKR4 regulates peripheral dendritic cell emigration. *Proc Natl Acad Sci U S A* **118**:e2025763118. doi:10.1073/pnas.2025763118

Blencowe BJ. 2017. The Relationship between Alternative Splicing and Proteomic Complexity. *Trends Biochem Sci* **42**:407–408. doi:10.1016/j.tibs.2017.04.001

Bond GL, Levine AJ. 2007. A single nucleotide polymorphism in the p53 pathway interacts with gender, environmental stresses and tumor genetics to influence cancer in humans. *Oncogene* **26**:1317–1323. doi:10.1038/sj.onc.1210199

Bourdon J-C, Fernandes K, Murray-Zmijewski F, Liu G, Diot A, Xirodimas DP, Saville MK, Lane DP. 2005. p53 isoforms can regulate p53 transcriptional activity. *Genes Dev* **19**:2122–2137. doi:10.1101/gad.1339905

Brayton CF, Treuting PM, Ward JM. 2012. Pathobiology of Aging Mice and GEM: Background Strains and Experimental Design. *Vet Pathol* **49**:85–105. doi:10.1177/0300985811430696

Calpe E, Codony C, Baptista MJ, Abrisqueta P, Carpio C, Purroy N, Bosch F, Crespo M. 2011. ZAP-70 enhances migration of malignant B lymphocytes toward CCL21 by inducing CCR7 expression via IgM-ERK1/2 activation. *Blood* **118**:4401–4410. doi:10.1182/blood-2011-01-333682

Chakraborty AA, Scuoppo C, Dey S, Thomas LR, Lorey SL, Lowe SW, Tansey WP. 2015. A common functional consequence of tumor-derived mutations within c-MYC. *Oncogene* **34**:2406–2409. doi:10.1038/onc.2014.186

Chow MT, Luster AD. 2014. Chemokines in cancer. *Cancer Immunol Res* **2**:1125–1131. doi:10.1158/2326-6066.CIR-14-0160

Courtois S, Verhaegh G, North S, Luciani M-G, Lassus P, Hibner U, Oren M, Hainaut P. 2002. DeltaN-p53, a natural isoform of p53 lacking the first transactivation domain, counteracts growth suppression by wild-type p53. *Oncogene* **21**:6722–6728. doi:10.1038/sj.onc.1205874

Danziger SA, McConnell M, Gockley J, Young MH, Rosenthal A, Schmitz F, Reiss DJ, Farmer P, Alapat DV, Singh A, Ashby C, Bauer M, Ren Y, Smith K, Couto SS, van Rhee F, Davies F, Zangari M, Petty N, Orlowski RZ, Dhodapkar MV, Copeland WB, Fox B, Hoering A, Fitch A, Newhall K, Barlogie B, Trotter MWB, Hershberg RM, Walker BA, Dervan AP, Ratushny AV, Morgan GJ. 2020. Bone marrow microenvironments that contribute to patient outcomes in newly diagnosed multiple myeloma: A cohort study of patients in the Total Therapy clinical trials. *PLoS Med* **17**:e1003323. doi:10.1371/journal.pmed.1003323

Duthu A, Debuire B, Romano J, Ehrhart JC, Fiscella M, May E, Appella E, May P. 1992. p53 mutations in Raji cells: characterization and localization relative to other Burkitt's lymphomas. *Oncogene* **7**:2161–2167.

Engeland K. 2018. Cell cycle arrest through indirect transcriptional repression by p53: I have a DREAM. *Cell Death Differ* **25**:114–132. doi:10.1038/cdd.2017.172

Feng L-Y, Ou Z-L, Wu F-Y, Shen Z-Z, Shao Z-M. 2009. Involvement of a novel chemokine decoy receptor CCX-CKR in breast cancer growth, metastasis and patient survival. *Clin Cancer Res* **15**:2962–2970. doi:10.1158/1078-0432.CCR-08-2495

Ferreira AC dos S, Robaina MC, Rezende LMM de, Severino P, Klumb CE. 2014. Histone deacetylase inhibitor prevents cell growth in Burkitt's lymphoma by regulating PI3K/Akt pathways and leads to upregulation of miR-143, miR-145, and miR-101. *Ann Hematol* **93**:983–993. doi:10.1007/s00277-014-2021-4

Flaman JM, Waridel F, Estreicher A, Vannier A, Limacher JM, Gilbert D, Iggo R, Frebourg T. 1996. The human tumour suppressor gene p53 is alternatively spliced in normal cells. *Oncogene* **12**:813–818.

Fornes O, Castro-Mondragon JA, Khan A, van der Lee R, Zhang X, Richmond PA, Modi BP, Correard S, Gheorghe M, Baranašić D, Santana-Garcia W, Tan G, Chèneby J, Ballester B, Parcy F, Sandelin A, Lenhard B, Wasserman WW, Mathelier A. 2020. JASPAR 2020: update of the open-access database of transcription factor binding profiles. *Nucleic Acids Res* **48**:D87–D92. doi:10.1093/nar/gkz1001

Georges A, L'Hôte D, Todeschini AL, Auguste A, Legois B, Zider A, Veitia RA. 2014. The transcription factor FOXL2 mobilizes estrogen signaling to maintain the identity of ovarian granulosa cells. *Elife* **3**:e04207. doi:10.7554/eLife.04207

Graubert TA, Shen D, Ding L, Okeyo-Owuor T, Lunn CL, Shao J, Krysiak K, Harris CC, Koboldt DC, Larson DE, McLellan MD, Dooling DJ, Abbott RM, Fulton RS, Schmidt H, Kalicki-Veizer J, O'Laughlin M, Grillot M, Baty J, Heath S, Frater JL, Nasim T, Link DC, Tomasson MH, Westervelt P, DiPersio JF, Mardis ER, Ley TJ, Wilson RK, Walter MJ. 2012. Recurrent mutations in the U2AF1 splicing factor in myelodysplastic syndromes. *Nat Genet* **44**:53–57. doi:10.1038/ng.1031

Haeussler M, Schönig K, Eckert H, Eschstruth A, Mianné J, Renaud J-B, Schneider-Maunoury S, Shkumatava A, Teboul L, Kent J, Joly J-S, Concordet J-P. 2016. Evaluation of off-target and on-target scoring algorithms and integration into the guide RNA selection tool CRISPOR. *Genome Biol* **17**:148. doi:10.1186/s13059-016-1012-2

Hamard P-J, Barthelery N, Hogstad B, Mungamuri SK, Tonnessen CA, Carvajal LA, Senturk E, Gillespie V, Aaronson SA, Merad M, Manfredi JJ. 2013. The C terminus of p53 regulates gene expression by multiple mechanisms in a target- and tissue-specific manner in vivo. *Genes Dev* **27**:1868–1885. doi:10.1101/gad.224386.113

Hamlyn PH, Rabbitts TH. 1983. Translocation joins c-myc and immunoglobulin gamma 1 genes in a Burkitt lymphoma revealing a third exon in the c-myc oncogene. *Nature* **304**:135–139. doi:10.1038/304135a0

Haupt S, Caramia F, Herschtal A, Soussi T, Lozano G, Chen H, Liang H, Speed TP, Haupt Y. 2019. Identification of cancer sex-disparity in the functional integrity of p53 and its X chromosome network. *Nat Commun* **10**:5385. doi:10.1038/s41467-019-13266-3

Hou T, Liang D, Xu L, Huang X, Huang Y, Zhang Y. 2013. Atypical chemokine receptors predict lymph node metastasis and prognosis in patients with cervical squamous cell cancer. *Gynecol Oncol* **130**:181–187. doi:10.1016/j.ygyno.2013.04.015

Hummel M, Bentink S, Berger H, Klapper W, Wessendorf S, Barth TFE, Bernd H-W, Cogliatti SB, Dierlamm J, Feller AC, Hansmann M-L, Haralambieva E, Harder L, Hasenclever D, Kühn M, Lenze D, Lichter P, Martin-Subero JI, Möller P, Müller-Hermelink H-K, Ott G, Parwaresch RM, Pott C, Rosenwald A, Rosolowski M, Schwaenen C, Stürzenhofecker B, Szczepanowski M, Trautmann H, Wacker H-H, Spang R, Loeffler M, Trümper L, Stein H, Siebert R, Molecular Mechanisms in Malignant Lymphomas Network Project of the Deutsche Krebshilfe. 2006. A biologic definition of Burkitt's lymphoma from transcriptional and genomic profiling. *N Engl J Med* **354**:2419–2430. doi:10.1056/NEJMoa055351

Ju Y, Sun C, Wang X. 2019. Loss of atypical chemokine receptor 4 facilitates C-C motif chemokine ligand 21-mediated tumor growth and invasion in nasopharyngeal carcinoma. *Exp Ther Med* **17**:613–620. doi:10.3892/etm.2018.7007

Kara EE, Bastow CR, McKenzie DR, Gregor CE, Fenix KA, Babb R, Norton TS, Zotos D, Rodda LB, Hermes JR, Bourne K, Gilchrist DS, Nibbs RJ, Alsharifi M, Vinuesa CG, Tarlinton DM, Brink R, Hill GR, Cyster JG, Comerford I, McColl SR. 2018. Atypical chemokine receptor 4 shapes activated B cell fate. *J Exp Med* **215**:801–813. doi:10.1084/jem.20171067

Kastan MB, Zhan Q, el-Deiry WS, Carrier F, Jacks T, Walsh WV, Plunkett BS, Vogelstein B, Fornace AJ. 1992. A mammalian cell cycle checkpoint pathway utilizing p53 and GADD45 is defective in ataxia-telangiectasia. *Cell* **71**:587–597. doi:10.1016/0092-8674(92)90593-2

Knewtson KE, Gonzalez Flores JG, Pacicca DM, Robinson JL. 2020. Transcriptome sequencing reveals sex differences in Human meniscal cell response to estrogen based on dosing kinetics (preprint). Genomics. doi:10.1101/2020.04.27.064451

Lacy SE, Barrans SL, Beer PA, Painter D, Smith AG, Roman E, Cooke SL, Ruiz C, Glover P, Van Hoppe SJL, Webster N, Campbell PJ, Tooze RM, Patmore R, Burton C, Crouch S, Hodson DJ. 2020. Targeted sequencing in DLBCL, molecular subtypes, and outcomes: a Haematological Malignancy Research Network report. *Blood* **135**:1759–1771. doi:10.1182/blood.2019003535

Langdon WY, Harris AW, Cory S, Adams JM. 1986. The c-myc oncogene perturbs B lymphocyte development in Eμ-myc transgenic mice. *Cell* **47**:11–18. doi:10.1016/0092-8674(86)90361-2

Liao Y, Smyth GK, Shi W. 2014. featureCounts: an efficient general purpose program for assigning sequence reads to genomic features. *Bioinformatics* **30**:923–930. doi:10.1093/bioinformatics/btt656

Love MI, Huber W, Anders S. 2014. Moderated estimation of fold change and dispersion for RNA-seq data with DESeq2. *Genome Biol* **15**:550. doi:10.1186/s13059-014-0550-8

Lowe SW, Schmitt EM, Smith SW, Osborne BA, Jacks T. 1993. p53 is required for radiation-induced apoptosis in mouse thymocytes. *Nature* **362**:847–849. doi:10.1038/362847a0

Mahani A, Arvidsson G, Sadeghi L, Grandien A, Wright APH. 2021. Differential transcriptional reprogramming by wild type and lymphoma-associated mutant MYC proteins as B-Cells convert to a lymphoma phenotype. *Cancers (Basel)* **13**:6093. doi:10.3390/cancers13236093

Maier B, Gluba W, Bernier B, Turner T, Mohammad K, Guise T, Sutherland A, Thorner M, Scrable H. 2004. Modulation of mammalian life span by the short isoform of p53. *Genes Dev* **18**:306–319. doi:10.1101/gad.1162404

Marcel V, Dichtel-Danjoy M-L, Sagne C, Hafsi H, Ma D, Ortiz-Cuaran S, Olivier M, Hall J, Mollereau B, Hainaut P, Bourdon J-C. 2011. Biological functions of p53 isoforms through evolution: lessons from animal and cellular models. *Cell Death Differ* **18**:1815–1824. doi:10.1038/cdd.2011.120

Marcuzzi E, Angioni R, Molon B, Calì B. 2018. Chemokines and Chemokine Receptors: Orchestrating Tumor Metastasization. *Int J Mol Sci* **20**:E96. doi:10.3390/ijms20010096

Martin M, Maßhöfer L, Temming P, Rahmann S, Metz C, Bornfeld N, van de Nes J, Klein-Hitpass L, Hinnebusch AG, Horsthemke B, Lohmann DR, Zeschnigk M. 2013. Exome sequencing identifies recurrent somatic mutations in EIF1AX and SF3B1 in uveal melanoma with disomy 3. *Nat Genet* **45**:933–936. doi:10.1038/ng.2674

Mondal AM, Horikawa I, Pine SR, Fujita K, Morgan KM, Vera E, Mazur SJ, Appella E, Vojtesek B, Blasco MA, Lane DP, Harris CC. 2013. p53 isoforms regulate aging- and tumor-associated replicative senescence in T lymphocytes. *J Clin Invest* **123**:5247–5257. doi:10.1172/JCI70355

Morin RD, Mendez-Lago M, Mungall AJ, Goya R, Mungall KL, Corbett RD, Johnson NA, Severson TM, Chiu R, Field M, Jackman S, Krzywinski M, Scott DW, Trinh DL, Tamura-Wells J, Li S, Firme MR, Rogic S, Griffith M, Chan S, Yakovenko O, Meyer IM, Zhao EY, Smailus D, Moksa M, Chittaranjan S, Rimsza L, Brooks-Wilson A, Spinelli JJ, Ben-Neriah S, Meissner B, Woolcock B, Boyle M, McDonald H, Tam A, Zhao Y, Delaney A, Zeng T, Tse K, Butterfield Y, Birol I, Holt R, Schein J, Horsman DE, Moore R, Jones SJM, Connors JM, Hirst M, Gascoyne RD, Marra MA. 2011. Frequent mutation of histone-modifying genes in non-Hodgkin lymphoma. *Nature* **476**:298–303. doi:10.1038/nature10351

Müller A, Homey B, Soto H, Ge N, Catron D, Buchanan ME, McClanahan T, Murphy E, Yuan W, Wagner SN, Barrera JL, Mohar A, Verástegui E, Zlotnik A. 2001. Involvement of chemokine receptors in breast cancer metastasis. *Nature* **410**:50–56. doi:10.1038/35065016

Oki S, Ohta T, Shioi G, Hatanaka H, Ogasawara O, Okuda Y, Kawaji H, Nakaki R, Sese J, Meno C. 2018. Ch IP □Atlas: a data□mining suite powered by full integration of public Ch IP □seq data. *EMBO Rep* **19**. doi:10.15252/embr.201846255

Pajares MJ, Ezponda T, Catena R, Calvo A, Pio R, Montuenga LM. 2007. Alternative splicing: an emerging topic in molecular and clinical oncology. *Lancet Oncol* **8**:349–357. doi:10.1016/S1470-2045(07)70104-3

Peuget S, Selivanova G. 2021. p53-Dependent Repression: DREAM or Reality? *Cancers* **13**:4850. doi:10.3390/cancers13194850

Pulvertaft RJV. 1964. Cytology of Burkitt's tumour (African Lymphoma). *The Lancet* **283**:238–240. doi:10.1016/S0140-6736(64)92345-1

Qin S, Li B, Li R, Cai Y, Zheng K, Huang H, Xiao F, Zeng M, Xu X. 2021. Proteomic characteristics and identification of PM2.5-induced differentially expressed proteins in hepatocytes and c-Myc silenced hepatocytes. *Ecotoxicol Environ Saf* **209**:111838. doi:10.1016/j.ecoenv.2020.111838

Rehm A, Mensen A, Schradi K, Gerlach K, Wittstock S, Winter S, Büchner G, Dörken B, Lipp M, Höpken UE. 2011. Cooperative function of CCR7 and lymphotoxin in the formation of a lymphoma-permissive niche within murine secondary lymphoid organs. *Blood* **118**:1020–1033. doi:10.1182/blood-2010-11-321265

Senturk S, Yao Z, Camiolo M, Stiles B, Rathod T, Walsh AM, Nemajerova A, Lazzara MJ, Altorki NK, Krainer A, Moll UM, Lowe SW, Cartegni L, Sordella R. 2014. p53Ψ is a transcriptionally inactive p53 isoform able to reprogram cells toward a metastatic-like state. *Proc Natl Acad Sci USA* **111**:E3287-96. doi:10.1073/pnas.1321640111

Sette C, Paronetto MP. 2022. Somatic Mutations in Core Spliceosome Components Promote Tumorigenesis and Generate an Exploitable Vulnerability in Human Cancer. *Cancers* **14**:1827. doi:10.3390/cancers14071827

Shi J-Y, Yang L-X, Wang Z-C, Wang L-Y, Zhou J, Wang X-Y, Shi G-M, Ding Z-B, Ke A-W, Dai Z, Qiu S-J, Tang Q-Q, Gao Q, Fan J. 2015. CC chemokine receptor-like 1 functions as a tumour suppressor by impairing CCR7-related chemotaxis in hepatocellular carcinoma: CCRL1 inhibits HCC progression. *J Pathol* **235**:546–558. doi:10.1002/path.4450

Si M, Lang J. 2018. The roles of metallothioneins in carcinogenesis. *J Hematol Oncol* **11**:107. doi:10.1186/s13045-018-0645-x

Simeonova I, Jaber S, Draskovic I, Bardot B, Fang M, Bouarich-Bourimi R, Lejour V, Charbonnier L, Soudais C, Bourdon J-C, Huerre M, Londono-Vallejo A, Toledo F. 2013. Mutant mice lacking the p53 C-terminal domain model telomere syndromes. *Cell Rep* **3**:2046–2058. doi:10.1016/j.celrep.2013.05.028

Simeonova I, Lejour V, Bardot B, Bouarich-Bourimi R, Morin A, Fang M, Charbonnier L, Toledo F. 2012. Fuzzy Tandem Repeats Containing p53 Response Elements May Define Species-Specific p53 Target Genes. *PLoS Genet* **8**:e1002731. doi:10.1371/journal.pgen.1002731

Slatter TL, Ganesan P, Holzhauer C, Mehta R, Rubio C, Williams G, Wilson M, Royds JA, Baird MA, Braithwaite AW. 2010. p53-mediated apoptosis prevents the accumulation of progenitor B cells and B-cell tumors. *Cell Death Differ* **17**:540–550. doi:10.1038/cdd.2009.136

Steffens Reinhardt L, Zhang X, Wawruszak A, Groen K, De Iuliis GN, Avery-Kiejda KA. 2020. Good Cop, Bad Cop: Defining the Roles of Δ40p53 in Cancer and Aging. *Cancers (Basel)* **12**:E1659. doi:10.3390/cancers12061659

Subramanian A, Tamayo P, Mootha VK, Mukherjee S, Ebert BL, Gillette MA, Paulovich A, Pomeroy SL, Golub TR, Lander ES, Mesirov JP. 2005. Gene set enrichment analysis: A knowledge-based approach for interpreting genome-wide expression profiles. *Proc Natl Acad Sci USA* **102**:15545–15550. doi:10.1073/pnas.0506580102

Toledo F, Krummel KA, Lee CJ, Liu C-W, Rodewald L-W, Tang M, Wahl GM. 2006. A mouse p53 mutant lacking the proline-rich domain rescues Mdm4 deficiency and provides insight into the Mdm2-Mdm4-p53 regulatory network. *Cancer Cell* **9**:273–285. doi:10.1016/j.ccr.2006.03.014

Tress ML, Abascal F, Valencia A. 2017a. Alternative Splicing May Not Be the Key to Proteome Complexity. *Trends Biochem Sci* **42**:98–110. doi:10.1016/j.tibs.2016.08.008

Tress ML, Abascal F, Valencia A. 2017b. Most Alternative Isoforms Are Not Functionally Important. *Trends Biochem Sci* **42**:408–410. doi:10.1016/j.tibs.2017.04.002

Ule J, Blencowe BJ. 2019. Alternative Splicing Regulatory Networks: Functions, Mechanisms, and Evolution. *Molecular Cell* **76**:329–345. doi:10.1016/j.molcel.2019.09.017

Ulvmar MH, Werth K, Braun A, Kelay P, Hub E, Eller K, Chan L, Lucas B, Novitzky-Basso I, Nakamura K, Rülicke T, Nibbs RJB, Worbs T, Förster R, Rot A. 2014. The atypical chemokine receptor CCRL1 shapes functional CCL21 gradients in lymph nodes. *Nat Immunol* **15**:623–630. doi:10.1038/ni.2889

Vassilev LT, Vu BT, Graves B, Carvajal D, Podlaski F, Filipovic Z, Kong N, Kammlott U, Lukacs C, Klein C, Fotouhi N, Liu EA. 2004. In vivo activation of the p53 pathway by small-molecule antagonists of MDM2. *Science* **303**:844–848. doi:10.1126/science.1092472

Watts AO, Verkaar F, Van Der Lee MMC, Timmerman CAW, Kuijer M, Van Offenbeek J, Van Lith LHCJ, Smit MJ, Leurs R, Zaman GJR, Vischer HF. 2013. β-Arrestin Recruitment and G Protein Signaling by the Atypical Human Chemokine Decoy Receptor CCX-CKR. *Journal of Biological Chemistry* **288**:7169–7181. doi:10.1074/jbc.M112.406108

Weatheritt RJ, Sterne-Weiler T, Blencowe BJ. 2016. The ribosome-engaged landscape of alternative splicing. *Nat Struct Mol Biol* **23**:1117–1123. doi:10.1038/nsmb.3317

Yin Y, Stephen CW, Luciani MG, Fåhraeus R. 2002. p53 Stability and activity is regulated by Mdm2-mediated induction of alternative p53 translation products. *Nat Cell Biol* **4**:462–467. doi:10.1038/ncb801

Younger ST, Kenzelmann-Broz D, Jung H, Attardi LD, Rinn JL. 2015. Integrative genomic analysis reveals widespread enhancer regulation by p53 in response to DNA damage. *Nucleic Acids Res* **43**:4447–4462. doi:10.1093/nar/gkv284

Zhu Q, Chen H, Li X, Wang X, Yan H. 2022. JMJD2C mediates the MDM2/p53/IL5RA axis to promote CDDP resistance in uveal melanoma. *Cell Death Discov* **8**:227. doi:10.1038/s41420-022-00949-y

Zhu Y, Tang W, Liu Y, Wang G, Liang Z, Cui L. 2014. CCX-CKR expression in colorectal cancer and patient survival. *Int J Biol Markers* **29**:e40-48. doi:10.5301/jbm.5000057

Figure Legends

Figure 1. The loss of p53-AS isoforms does not alter cellular stress responses or survival to spontaneous tumors.

(**A**) mRNAs for p53-α and p53-AS isoforms from thymocytes of irradiated mice were quantified by RT-qPCR, and p53-α levels in $p53^{+/+}$ mice were assigned a value of 1. Means ± SEM (n=3). (**B**) Protein extracts from thymocytes of irradiated mice were immunoblotted with p53 or actin antibodies. After normalisation to actin, full-length (FL) p53-α levels in $p53^{+/+}$ thymocytes were assigned a value of 1. (**C**) mRNA levels of p53 target genes in thymocytes, before or after γ-irradiation. Means ± SEM (n=3). (**D**) Thymocyte apoptotic response to γ-irradiation. Means ± SEM (n=6). (**E**) Cell cycle control in mouse embryonic fibroblasts (MEFs) after γ-irradiation. Asynchronous MEFs were exposed to 0-10 Gy γ-irradiation, and after 24h, cells were labelled with BrdU for 1h and analyzed by FACS. Means ± SEM from >3 independent experiments with at least 2 independent MEF clones per genotype. (**F**) mRNA levels of p53 target genes in MEFs untreated or treated with 0.5 μg/ml of clastogenic Doxorubicin (Doxo) or 10 μM of the Mdm2 antagonist Nutlin. Means ± SEM from > 3 experiments with ≥ 2 independent MEF clones. (**G**) MEFs proliferation under hyperoxic conditions. Cells were grown according to a 3T3 protocol. Each point is the mean from 4 independent MEF clones, the value for each clone resulting from triplicates. (**H**) Growth of tumor xenografts. E1A+Ras-expressing MEFs were injected into the flanks of nude mice and tumor volumes were determined after 1-25 days. Means ± SD (n=4 per timepoint and genotype). (**I**) Tumor-free survival of $p53^{+/+}$ and $p53^{\Delta AS/\Delta AS}$ mice (n=cohort size). (**J**) Incidence of the indicated tumor types, determined at death after macroscopic examination and histological analysis. In A, D, E, ns=non-significant in Student's t-test.

Figure 2. Male-specific acceleration of Myc-induced B-cell lymphomagenesis in mice lacking p53-AS isoforms.

(**A**) Tumor-free survival of $p53^{+/+}$ Eμ-Myc and $p53^{\Delta AS/\Delta AS}$ Eμ-Myc mice, classified according to sex. (n=cohort size). (**B**) Tumor volumes upon dissection of $p53^{+/+}$ Eμ-Myc and $p53^{\Delta AS/\Delta AS}$ Eμ-Myc mice, classified according to sex. Means ± SEM from 100 lymph nodes from $p53^{+/+}$ Eμ-Myc males, 96 from $p53^{+/+}$ Eμ-Myc females, 148 from $p53^{\Delta AS/\Delta AS}$ Eμ-Myc males and 124 from $p53^{\Delta AS/\Delta AS}$ Eμ-Myc females. (**C**) Myc mRNA and protein levels in lymph node tumors. (**D**) Levels of p53-α and p53-AS transcripts and p53 protein levels in lymph node tumors. (**E**) Transcript levels of the indicated p53 target genes. Means ± SEM (n=6 per genotype). (**F-G**) Apoptosis (F) and cell proliferation (G) in tumor lymph nodes from Eμ-Myc males were determined by immunohistochemistry with antibodies against cleaved caspase-3 and ki67, respectively. Positive cells were counted and normalized to the analyzed areas. Means ± SEM (n=6 mice per assay and genotype). In F, G scale bars=50 μm. Statistical analyses with Mantel-Cox (A) and Student's t (B-G) tests. ***P<0.001, *P<0.05, ns: non-significant.

Figure 3. The loss of p53-AS isoforms affects *Ackr4* expression in Eμ-Myc male mice.
(**A**) B-cell subpopulations in spleens of 6 weeks-old $p53^{+/+}$ Eμ-Myc and $p53^{\Delta AS/\Delta AS}$ Eμ-Myc mice. Means ± SEM (n=6 per genotype). (**B-C**) RNAseq analysis of spleens from $p53^{+/+}$ Eμ-Myc (n=3) and $p53^{\Delta AS/\Delta AS}$ Eμ-Myc (n=4) 4-6 weeks-old male mice. Volcano plot (B), with differentially expressed genes (DEGs) in red. Unsupervised clustering heat-map plot (C), with DEGs ranked according to mean fold changes, and protein-coding genes in bold. (**D**) RT-qPCR analysis of candidate DEGs from spleens of $p53^{+/+}$ Eμ-Myc males and $p53^{\Delta AS/\Delta AS}$ Eμ-Myc males. Means ± SEM (n=3-4 per genotype). (**E**) RT-qPCR analysis of indicated DEGs from spleens of 4-6 weeks-old $p53^{+/+}$ Eμ-Myc males, $p53^{\Delta AS/\Delta AS}$ Eμ-Myc males, $p53^{+/+}$ Eμ-Myc females and $p53^{\Delta AS/\Delta AS}$ Eμ-Myc females. Means ± SEM (n=3-4 per sex and genotype). (**F**) *Ackr4* is transactivated by p53 in response to stress. Ackr4 mRNAs in untreated or doxorubicin-treated WT and $p53^{-/-}$ MEFs. Data from 2-3 MEFs per genotype (Younger et al., 2015). (**G**) A putative p53 response element in *Ackr4* intron 1. Top: Map of the *Ackr4* gene. (boxes: exons (brown box: translated region), black line: intron 1); middle: p53 ChIP in doxorubicin-treated MEFs according to ChIP-Atlas (SRX270554) (Oki et al., 2018); bottom: p53 Response Element (p53RE) consensus sequence (R=G or A, W=A or T, Y=C or T), the putative p53RE and its mutated counterpart. (**H**) Luciferase assays of the candidate p53RE. A 1.5 kb fragment containing the WT or mutant p53RE was cloned upstream a luciferase reporter, then transfected into $p53^{-/-}$ MEFs together with an expression plasmid for full length p53 (FL), p53-AS or the DNA-binding mutant $p53^{R270H}$ (RH). Means ± SEM (n=4-6). (**I**) In MEFs, p53 activation leads to an increased *Ackr4* expression attenuated by estradiol. *Ackr4* and *Cdkn1a* mRNAs were quantified by RT-qPCR from $p53^{+/+}$ and $p53^{\Delta AS/\Delta AS}$ MEFs, untreated or treated with 10 μM Nutlin and/or 5 μg/ml 17-β estradiol (E2). Means ± SEM from 4 independent experiments. (**J**) Evidence for Myc binding at the *Mt2* promoter in B-cells. ChIP-Atlas reports Myc binding to *Mt2* promoter sequences in primary B-cells from the lymph nodes of Eμ-Myc mice (SRX353785, SRX353783) and in Eμ-Myc-induced lymphoma cells (SRX522383). Chr: chromosome. (**K**) Gene set enrichment analysis (GSEA). GSEA, performed in $p53^{+/+}$ Eμ-Myc and $p53^{\Delta AS/\Delta AS}$ Eμ-Myc male splenic cells, indicated an enrichment of hallmark Myc targets in $p53^{\Delta AS/\Delta AS}$ Eμ-Myc cells. In A, D, E, F, H, I ***P<0.001, **P<0.01, *P<0.05, °P≤0.057, ns: non-significant in Student's t or Mann-Whitney tests.

Figure 4. *ACKR4* is a male-specific prognostic factor in Burkitt lymphoma.
(**A**) In human cells, p53 activation leads to an increased *ACKR4* expression abrogated by estradiol. *ACKR4* and *CDKN1A* mRNAs were quantified by RT-qPCR from p53-proficient (MRC5) and p53-deficient (MRC5-SV40) human fibroblasts, untreated or treated with Nutlin and/or estradiol (E2). Means ± SEM from 4 independent experiments. (**B-C**) Analysis of lymphoma dataset #GSE4475. *ACKR4* gene expression was plotted for all lymphoma patients with clinical follow-up (91 men [M], 68 women [W]), classified according to sex (B, left). Gene expression (B, right) or survival curves (C) were plotted for the 30% patients (27 men,

20 women) with the highest or lowest *ACKR4* expression, classified according to sex. (**D-E**) Analysis of Burkitt lymphoma-specific dataset #phs00235. *ACKR4* gene expression was plotted for all patients with a Burkitt lymphoma diagnosed at age 0-17 (48 males, 29 females), classified according to sex (D, left). Gene expression (D, right) or survival curves (E) were plotted for the 30% patients (15 men, 9 women) with the highest or lowest *ACKR4* expression, classified according to sex. (**F**) The knockout of *ACKR4* in Burkitt lymphoma Raji cells increases their CCL21-guided migration. Chemotaxis was assayed by using Boyden chambers with bare polycarbonate membranes as previously described (Calpe et al., 2011). Equal number of cells were deposited on the membrane of a transwell insert, then migration was determined by counting cells in the lower compartment, after 15h of culture with or without CCL21 added to the lower chamber. Statistical analyses by Student's t or Mann-Whitney tests (A, B, D, F) and Mantel-Cox (C, E) test. ***P<0.001, **P<0.01, * P<0.01, °P=0.054, ns: non-significant.

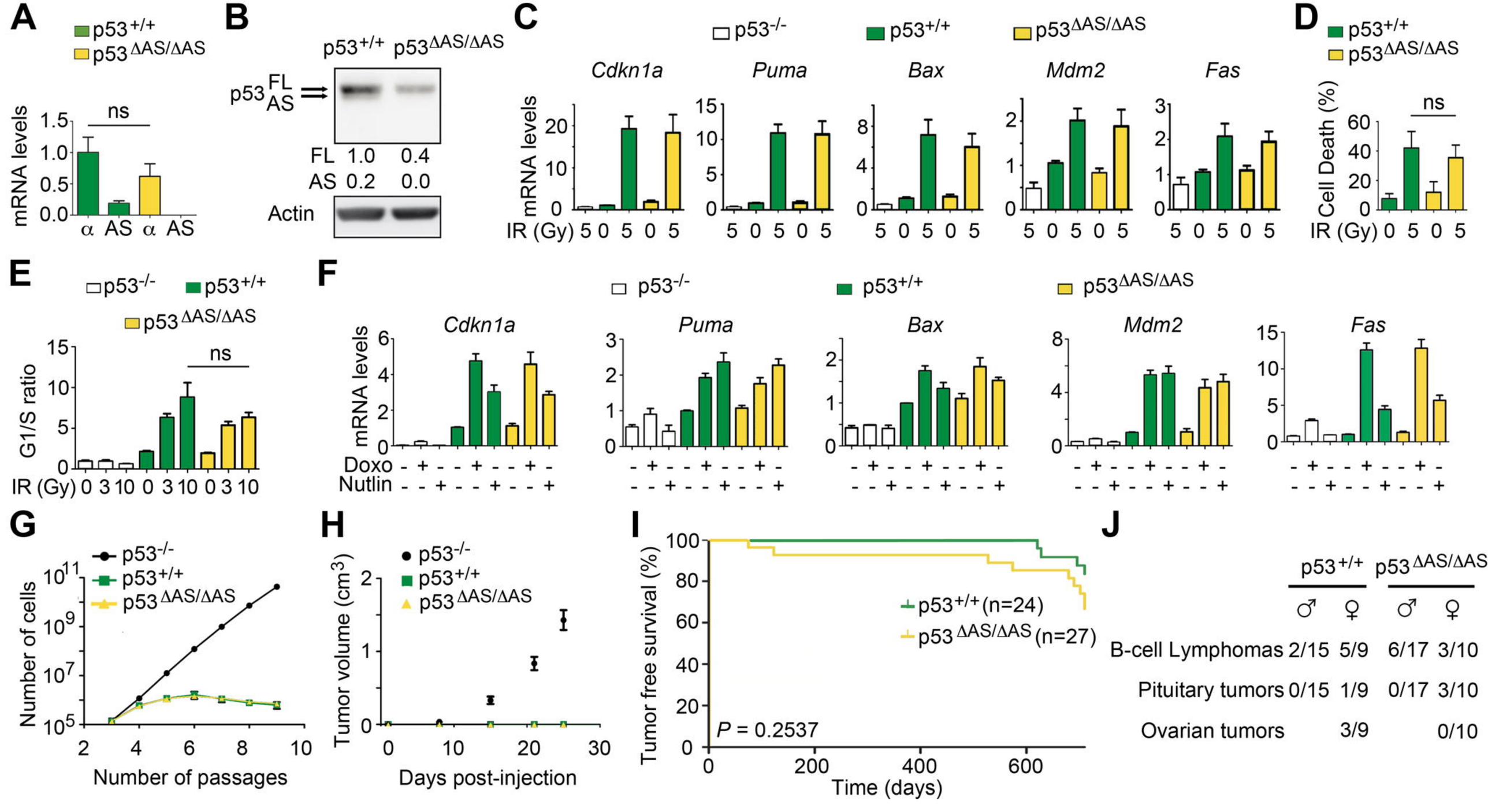
A
p53+/+
p53ΔAS/ΔAS
mRNA levels
ns
α AS α AS
B
p53+/+ p53ΔAS/ΔAS
p53 FL AS
FL 1.0 0.4
AS 0.2 0.0
Actin
C
p53-/-
p53+/+
p53ΔAS/ΔAS
Cdkn1a
Puma
Bax
Mdm2
Fas
mRNA levels
IR (Gy) 5 0 5 0 5
D
p53+/+
p53ΔAS/ΔAS
Cell Death (%)
ns
IR (Gy) 0 5 0 5
E
p53-/-
p53+/+
p53ΔAS/ΔAS
G1/S ratio
ns
IR (Gy) 0 3 10 0 3 10 0 3 10
F
p53-/-
p53+/+
p53ΔAS/ΔAS
Cdkn1a
Puma
Bax
Mdm2
Fas
mRNA levels
Doxo
Nutlin
G
p53-/-
p53+/+
p53ΔAS/ΔAS
Number of cells
Number of passages
H
p53-/-
p53+/+
p53ΔAS/ΔAS
Tumor volume (cm3)
Days post-injection
I
p53+/+ (n=24)
p53ΔAS/ΔAS (n=27)
Tumor free survival (%)
P = 0.2537
Time (days)
J
p53+/+ p53ΔAS/ΔAS
♂ ♀ ♂ ♀
B-cell Lymphomas 2/15 5/9 6/17 3/10
Pituitary tumors 0/15 1/9 0/17 3/10
Ovarian tumors 3/9 0/10

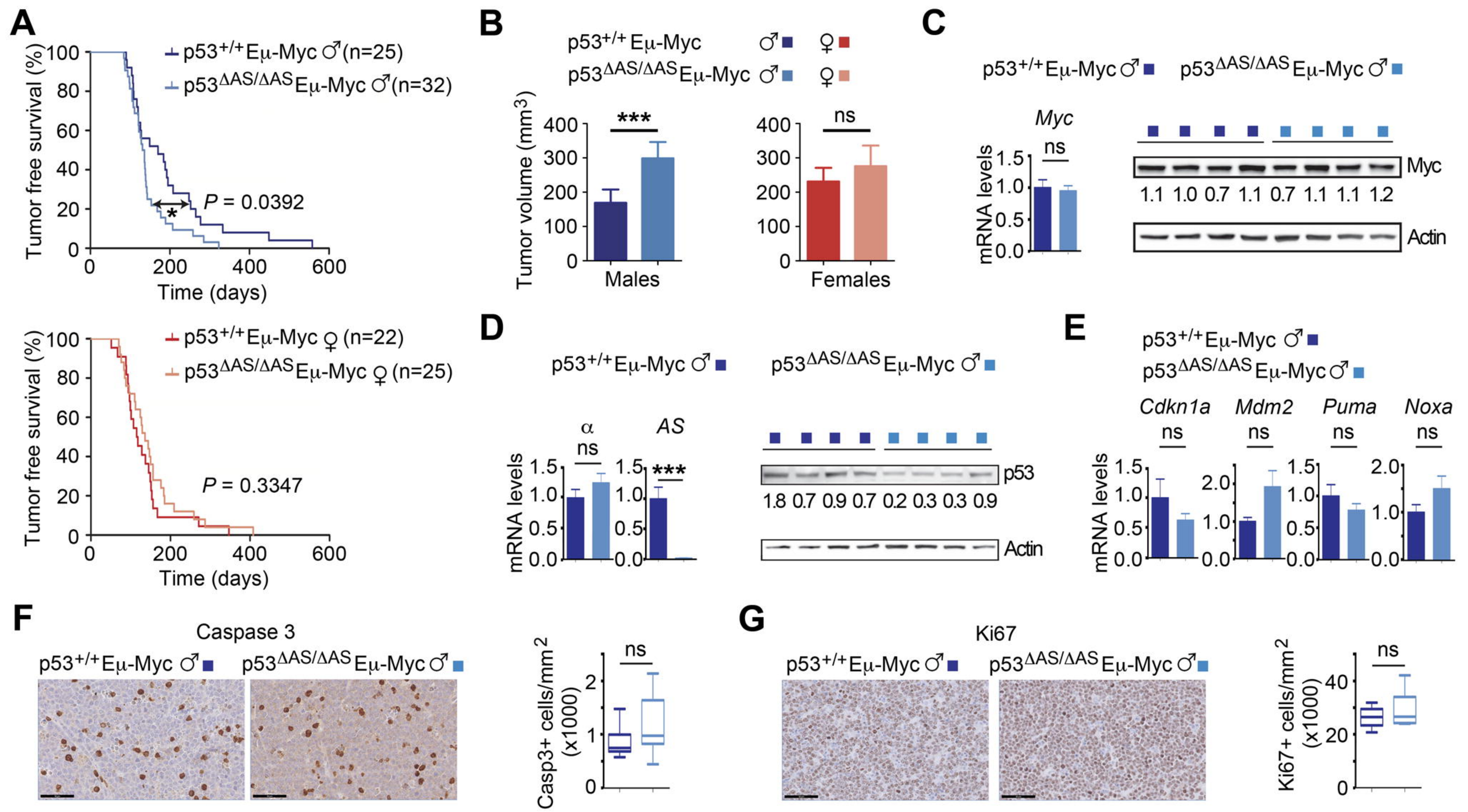
A
Tumor free survival (%)
p53+/+Eμ-Myc ♂(n=25)
p53ΔAS/ΔASEμ-Myc ♂(n=32)
P = 0.0392
*
Time (days)
p53+/+Eμ-Myc ♀ (n=22)
p53ΔAS/ΔASEμ-Myc ♀ (n=25)
P = 0.3347
B
p53+/+ Eμ-Myc ♂ ♀
p53ΔAS/ΔASEμ-Myc ♂ ♀
Tumor volume (mm3)
***
ns
Males
Females
C
p53+/+Eμ-Myc ♂
p53ΔAS/ΔASEμ-Myc ♂
Myc
ns
mRNA levels
Myc
1.1 1.0 0.7 1.1 0.7 1.1 1.1 1.2
Actin
D
p53+/+Eμ-Myc ♂
p53ΔAS/ΔASEμ-Myc ♂
α
AS
ns
***
mRNA levels
p53
1.8 0.7 0.9 0.7 0.2 0.3 0.3 0.9
Actin
E
p53+/+Eμ-Myc ♂
p53ΔAS/ΔASEμ-Myc ♂
Cdkn1a
Mdm2
Puma
Noxa
ns
mRNA levels
F
Caspase 3
p53+/+Eμ-Myc ♂
p53ΔAS/ΔASEμ-Myc ♂
Casp3+ cells/mm2 (x1000)
ns
G
Ki67
p53+/+Eμ-Myc ♂
p53ΔAS/ΔASEμ-Myc ♂
Ki67+ cells/mm2 (x1000)
ns

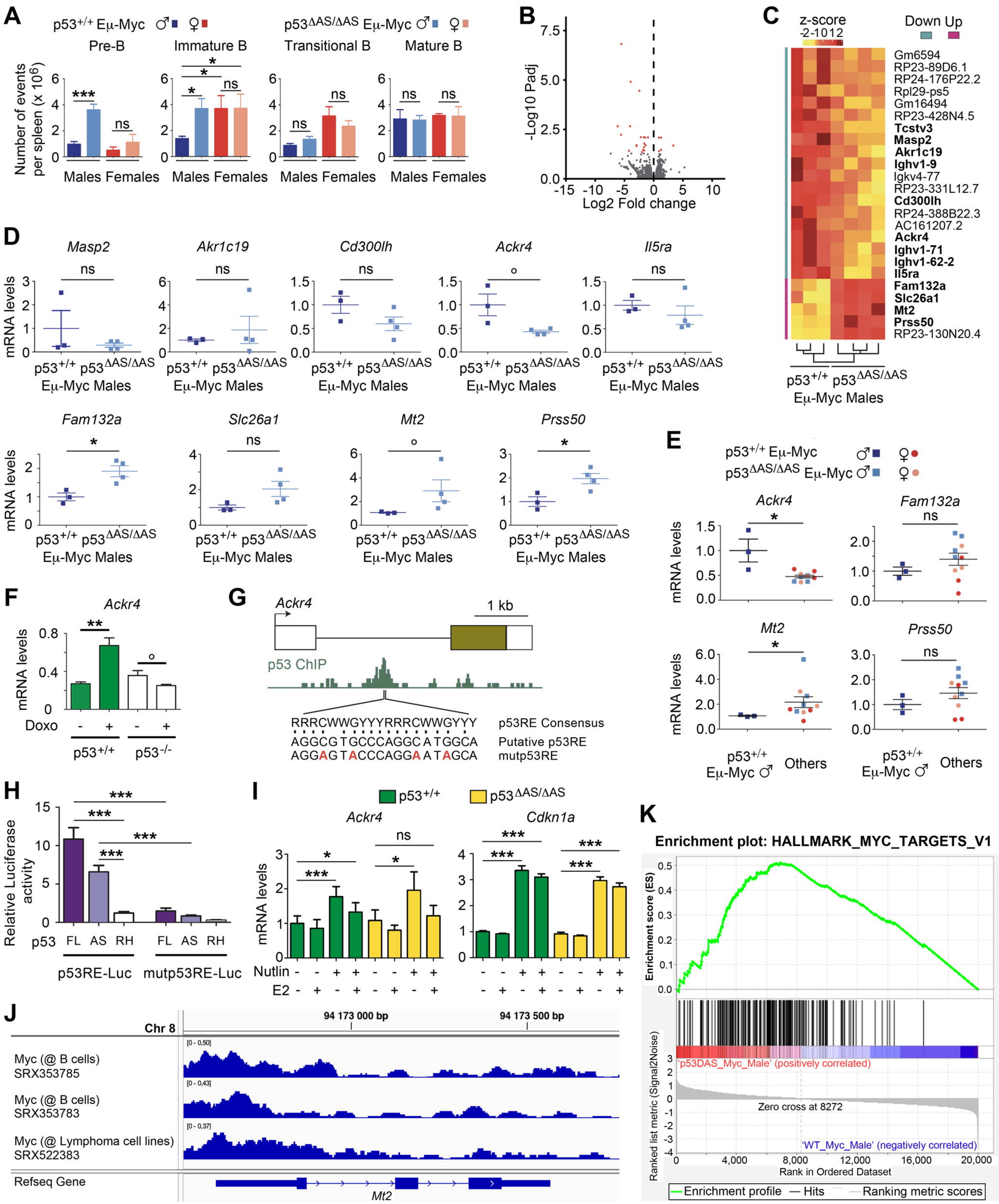
A
p53+/+ Eμ-Myc ♂ ♀
p53ΔAS/ΔAS Eμ-Myc ♂ ♀
Pre-B
Immature B
Transitional B
Mature B
Number of events per spleen (x 10^6)
Males Females
B
-Log10 Padj
Log2 Fold change
C
z-score
Down Up
Gm6594
RP23-89D6.1
RP24-176P22.2
Rpl29-ps5
Gm16494
RP23-428N4.5
Tcstv3
Masp2
Akr1c19
Ighv1-9
Igkv4-77
RP23-331L12.7
Cd300lh
RP24-388B22.3
AC161207.2
Ackr4
Ighv1-71
Ighv1-62-2
Il5ra
Fam132a
Slc26a1
Mt2
Prss50
RP23-130N20.4
p53+/+ p53ΔAS/ΔAS
Eμ-Myc Males
D
Masp2
Akr1c19
Cd300lh
Ackr4
Il5ra
Fam132a
Slc26a1
Mt2
Prss50
mRNA levels
p53+/+ p53ΔAS/ΔAS
Eμ-Myc Males
E
p53+/+ Eμ-Myc ♂ ♀
p53ΔAS/ΔAS Eμ-Myc ♂ ♀
Ackr4
Fam132a
Mt2
Prss50
mRNA levels
p53+/+ Eμ-Myc ♂
Others
F
Ackr4
mRNA levels
Doxo
p53+/+
p53-/-
G
Ackr4
1 kb
p53 ChIP
RRRCWWGYYYRRRCWWGYYY
AGGCGTGCCCAGGCATGGCA
AGGAGTACCCAGGAATAGCA
p53RE Consensus
Putative p53RE
mutp53RE
H
Relative Luciferase activity
p53 FL AS RH FL AS RH
p53RE-Luc
mutp53RE-Luc
I
p53+/+
p53ΔAS/ΔAS
Ackr4
Cdkn1a
mRNA levels
Nutlin
E2
J
Chr 8
94 173 000 bp
94 173 500 bp
Myc (@ B cells) SRX353785
Myc (@ B cells) SRX353783
Myc (@ Lymphoma cell lines) SRX522383
Refseq Gene
Mt2
K
Enrichment plot: HALLMARK_MYC_TARGETS_V1
Enrichment score (ES)
'p53DAS_Myc_Male' (positively correlated)
Zero cross at 8272
'WT_Myc_Male' (negatively correlated)
Ranked list metric (Signal2Noise)
Rank in Ordered Dataset
Enrichment profile
Hits
Ranking metric scores

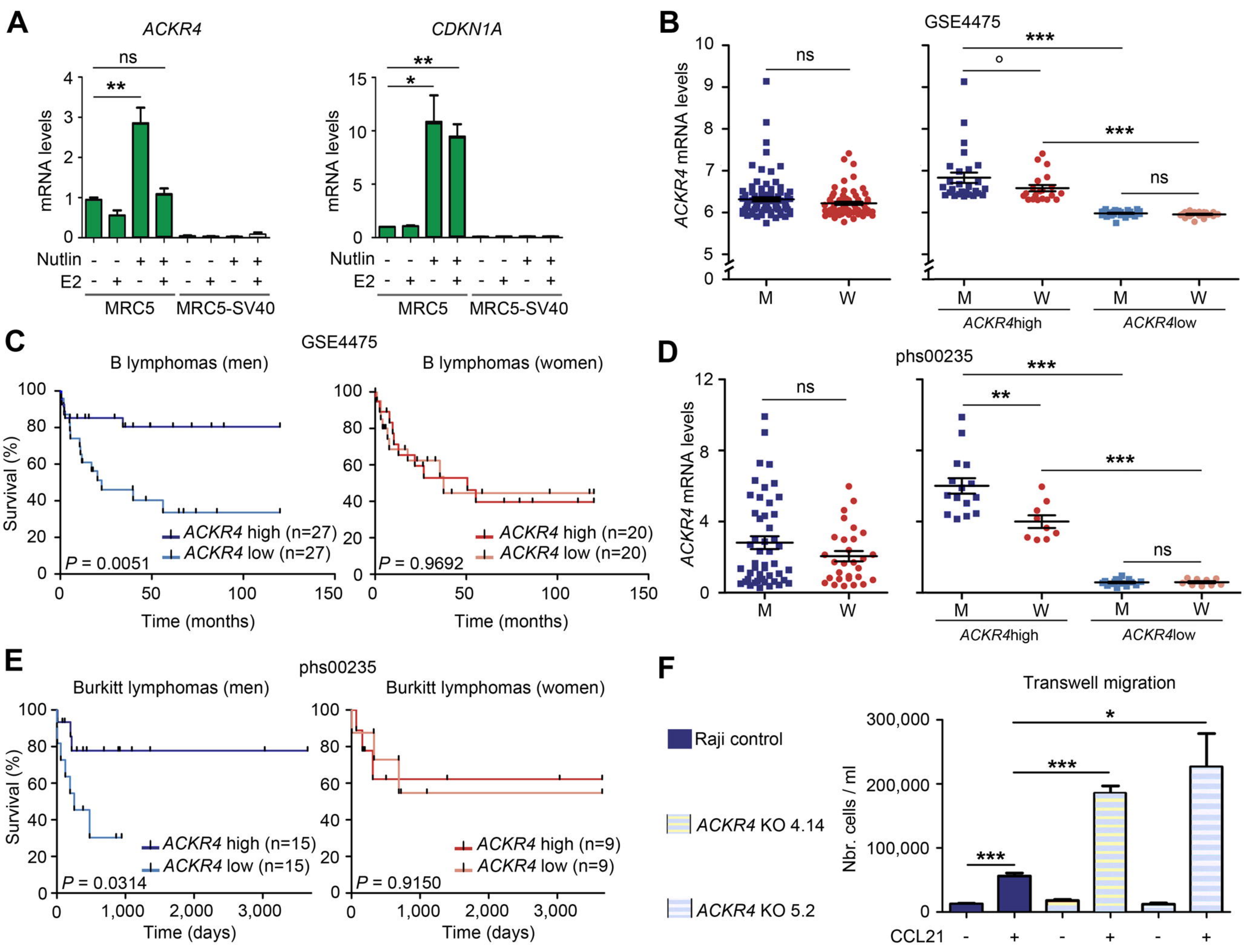
A
ACKR4
CDKN1A
mRNA levels
ns
**
*
Nutlin
E2
MRC5
MRC5-SV40
B
GSE4475
ACKR4 mRNA levels
M
W
ACKR4high
ACKR4low
C
GSE4475
B lymphomas (men)
B lymphomas (women)
Survival (%)
Time (months)
ACKR4 high (n=27)
ACKR4 low (n=27)
P = 0.0051
ACKR4 high (n=20)
ACKR4 low (n=20)
P = 0.9692
D
phs00235
E
phs00235
Burkitt lymphomas (men)
Burkitt lymphomas (women)
Time (days)
ACKR4 high (n=15)
ACKR4 low (n=15)
P = 0.0314
ACKR4 high (n=9)
ACKR4 low (n=9)
P = 0.9150
F
Transwell migration
Raji control
ACKR4 KO 4.14
ACKR4 KO 5.2
Nbr. cells / ml
CCL21